Appl. Phys. B 81, 459–464 (2005)
DOI: 10.1007/s00340-005-1926-y

Applied Physics B
Lasers and Optics

Y. XIA
L. DENG
J. YIN✉

Electrostatic guiding of cold polar molecules on a chip

Key Laboratory of Optical and Magnetic Resonance Spectroscopy, Department of Physics, East China Normal University, Shanghai 200062, P.R. China

Received: 25 January 2005 / Final version: 14 June 2005
Published online: 29 July 2005 •

ABSTRACT We propose a novel scheme to guide cold polar molecules on the surface of an insulating substrate (i.e. a chip) using an electrostatic field generated by the combination of a pair of parallel charged wires and a grounded metal plate. The spatial distributions of the electric fields from the above charged-wire layout and their Stark potentials for cold CO molecules and dipole forces are calculated, and the relationships between the electric field and the geometric parameters of our charged-wire system are analyzed. Our study shows that our charged-wire scheme can be used to guide cold polar molecules in the weak-field-seeking state, and to construct various molecular optical elements, such as a molecular funnel, a molecular beam splitter and a molecular interferometer and so on, to form various integrated molecular optical elements and their molecular chips, and even to generate a continuous wave (CW) cold molecular beam by using a low-pass energy filter based on bent two-wire guiding.

PACS 33.80.Ps; 33.55.Be; 39.10.+j

1 Introduction

In recent years, cold molecules with rich internal level structure have opened up some new opportunities for molecular precision spectroscopy and measurements [1, 2], studies of cold molecular collisions [3–8], quantum information processing [9] and so on. Until now, the main techniques to prepare cold or ultra-cold molecules are of three types, namely buffer-gas cooling of paramagnetic molecules [10, 11], photoassociation of pre-cooled atoms in a magneto-optical trap [12–22] or in a Bose–Einstein condensation [23–25] and Stark deceleration of supersonic polar molecules [26–31]. More recently, a single-stage optical Stark decelerator for benzene molecules has been demonstrated; this technique relies on the second-order Stark interaction between the molecules and the intense laser field [32].

In 2000, Loesch and Scheel demonstrated the Keppler-type electrostatic guiding of polar molecules (NaCl, NaBr, NaI) in the strong-field-seeking state [33]. Since the molecules in the injected polar molecular beam that can satisfy the Keppler motion orbit are very small in number, the electrostatic guiding efficiency of strong-field-seeking molecules is very low. For example, the maximum guiding efficiency for NaBr molecules is only $\sim 0.12\%$ in Loesch and Scheel's experiment. Recently, an electrostatic bent guiding technique was used to produce a continuous cold polar molecular beam (H_2CO, ND_3) in the weak- or strong-field-seeking state by using a two-dimensional (2D) quadrupole electrostatic or time-varying electric field, which is generated by four identical bent charged electrodes [34–36]. It is clear that the 2D Gaussian-like electrostatic field (i.e. Keppler guide) [33], a hollow electrostatic one [34, 36] or even a 2D time-varying Gaussian-like ac electric field [35] cannot only be used to guide, manipulate and control cold molecules in the weak- or strong-field-seeking state, but also to generate a cold molecular beam by using a low-pass energy filter based on the bent molecular guiding. However, these guiding schemes cannot be used to realize surface guiding of cold molecules on a substrate (i.e. a chip). So, it would be interesting and worthwhile to find a highly efficient guiding scheme and realize electrostatic surface guiding of cold polar molecules in the weak-field-seeking state on a molecular chip.

In this paper, we propose a novel and simple scheme to guide cold polar molecules on the surface of an insulating substrate (i.e. a chip) using a hollow electrostatic field generated by the combination of a pair of parallel charged wires and a grounded metal plate, study the spatial distributions of the electrostatic field and discuss some potential applications of our surface guiding scheme in molecular optics. In Sect. 2, we introduce the electrostatic surface guiding scheme for cold polar molecules in the weak-field-seeking state, and derive the equations to calculate the electric field distribution from the charged-wire layout and its distribution of the Stark trapping potential. In Sect. 3, the spatial distributions of the electric field from our charged two-wire layout and their Stark trapping potentials for cold CO molecules are calculated, and the relationships between the electric field (including trapping potential and force) and the parameters of the electrostatic guiding system are analyzed. In Sect. 4, the loading of guided cold molecules, some potential applications of our two-wire guiding scheme and its advantages are briefly discussed. Some main results and conclusions are summarized in Sect. 5.

✉ Fax: +86-021-62232056, E-mail: jpyin@phy.ecnu.edu.cn

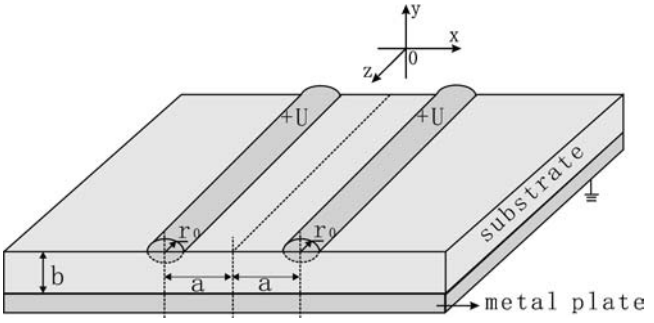

FIGURE 1 Schematic diagram of molecular surface electrostatic guiding using a static electric field generated by the combination of two charged wires (i.e. two parallel stainless steel rods) on the insulating substrate and the grounded metal plate. The radius of the cylindrical wire is r_0, the center-to-center separation of the two wires is $2a$ and the distance between a wire center and the grounded metal plate is b; a positive voltage ($+U$) is applied to the two wires

2 Surface guiding scheme and derivation of formulas

Our guiding scheme is shown in Fig. 1 and consists of two parallel charged wires (i.e. two cylindrical stainless steel rods) on the surface of an insulating substrate and a grounded metal plate. Here the wire radius is r_0, the space between the centers of the two wires is $2a$ and the distance from a wire center to the grounded metal plate is b; the relative dielectric constant of the selected insulating material is ε_r. A high-voltage source with a voltage $+U$ is applied to both the wires and used to produce a hollow quadrupole electrostatic field distribution with a central minimum, so as to realize the electrostatic guiding of cold polar molecules in the weak-field-seeking state on the substrate surface. To eliminate the effect of Majorana transitions, a low voltage U' applied between two infinite transparent electrodes of a plate capacitor is used to produce a weak homogeneous bias field $\mathbf{E}_0$ along the z direction. In order to let an incident molecular beam enter our two-wire guiding system, the center of each electrode of the plate capacitor has a small hole with a radius of 1 mm.

Let us assume that the charged wires are infinitely long in the z direction. According to the Poisson equation and method of images (i.e. the image charge method) [37], we can derive the following equations to calculate the electric field distribution in free space generated by our charged-wire system:

$$E_\mathrm{x} = \frac{2U}{C(\varepsilon_\mathrm{r}+1)}\left[\frac{x-a_1}{(x-a_1)^2+(y-b_1)^2} - \frac{x-a_1}{(x-a_1)^2+(y-b_2)^2} + \frac{x-a_2}{(x-a_2)^2+(y-b_1)^2} - \frac{x-a_2}{(x-a_2)^2+(y-b_2)^2}\right], \tag{1}$$

$$E_\mathrm{y} = \frac{2U}{C(\varepsilon_\mathrm{r}+1)}\left[\frac{y-b_1}{(x-a_1)^2+(y-b_1)^2} - \frac{y-b_1}{(x-a_1)^2+(y-b_2)^2} + \frac{y-b_2}{(x-a_2)^2+(y-b_1)^2} - \frac{y-b_2}{(x-a_2)^2+(y-b_2)^2}\right], \tag{2}$$

where C is a constant, and we have

$$a_1 = \sqrt{a^2+r_0^2} - \left(\sqrt{a^2+b^2} - \sqrt{a^2+b^2-r_0^2}\right) \times \frac{a}{\sqrt{a^2+b^2}}, \quad a_2 = -a_1, \tag{3}$$

$$b_1 = -\left[\left(b - \sqrt{b^2-r_0^2}\right) + \left(\sqrt{a^2+b^2} - \sqrt{a^2+b^2-r_0^2}\right) \times \frac{a}{\sqrt{a^2+b^2}}\right], \quad b_2 = -2b - b_1, \tag{4}$$

and then the total electric field distribution is given by

$$|\mathbf{E}(x,y)| = \sqrt{E_\mathrm{x}^2(x,y) + E_\mathrm{y}^2(x,y)}. \tag{5}$$

From Eqs. (1)–(5), we can calculate the spatial distribution of the electric field $|E(x,y)|$ in free space from our charged-wire layout, and analyze the relationships between the electric field distribution $|E(x,y)|$ and the geometric parameters (a, b and r_0) of our guiding system.

We know that when a polar molecule with a permanent electric dipole moment (EDM) $\boldsymbol{\mu}$ moves in an inhomogeneous electrostatic field, due to the first-order Stark effect, it will feel a dipole gradient force from the electrostatic field, which can be used to realize the electrostatic guiding or trapping of cold polar molecules.

When the angle θ between the EDM and the external electric field $\mathbf{E}$ is fixed, we can introduce an effective dipole moment $\mu_\mathrm{eff} = \mu\langle\cos\theta\rangle$, where μ is the magnitude of the permanent EDM and $\langle\cos\theta\rangle$ represents the quantum-mechanical averaging over all angles. In consideration of the interaction of a polar molecule (with a permanent EDM) with an inhomogeneous electrostatic field $\mathbf{E}$, the interacting Stark potential for cold polar molecules can be written as

$$W_\mathrm{Stark} = -\boldsymbol{\mu}\cdot\mathbf{E}. \tag{6}$$

We find from Eq. (6) that when the average orientation of the molecular EDM is parallel to the electric field $\mathbf{E}$, that is, when $\boldsymbol{\mu}\cdot\mathbf{E}$ is positive, the Stark potential is attractive, and the molecule in the strong-field-seeking state will be attracted to the maximum of the electrostatic field, which can be used to guide the strong-field-seeking molecules around the charged wire [33]. When the average orientation of the molecular EDM is anti-parallel to the electrostatic field $\mathbf{E}$, i.e. when $\boldsymbol{\mu}\cdot\mathbf{E}$ is negative, the Stark potential is repulsive, and the molecules in the weak-field-seeking state will be repelled to the minimum of the electric field, which can be used to realize the electrostatic guiding (i.e. two-dimensional trapping) of cold weak-field-seeking molecules [34–36].

For a CO molecule in the metastable $a^3\Pi$ ($J=1$, $M\Omega=-1$) state, it has a relatively large EDM with 1.37 Debye (4.6×10^{-30} C m) and a strong first-order Stark effect and when the electric field used to guide the CO molecule is lower than 50 kV/cm, the second-order Stark effect can be neglected; the confining potential for the CO molecule, due to the first-order Stark effect, is then given by

$$W_\mathrm{Stark} = -\mu_\mathrm{eff}\,|\mathbf{E}| \tag{7}$$

and the corresponding dipole gradient force from the electrostatic field, acting on the cold polar molecules, is given by

$$\mathbf{F} = -\nabla W_{\text{Stark}} = \mu_{\text{eff}} \nabla \mathbf{E}. \tag{8}$$

It is clear that when μ_{eff} is negative, the weak-field-seeking molecules will be repelled to the minimum of the electric field by the repulsive gradient force $\mathbf{F}$.

3 Theoretical calculations and analysis

From Eqs. (1)–(5), we calculate the contours of the electric field $|\mathbf{E}|$ in free space generated by the charged-wire layout in Fig. 1, and the result is similar to those in Fig. 5c. We find from Fig. 5c that there is a point of zero electric field on the y axis, and its coordinate position (the guiding center) is at $(0, y_0)$, which is like a hollow electrostatic tube with a point $|\mathbf{E}| = 0$ at the position $(0, y_0)$ and can be used to guide cold polar molecules in the weak-field-seeking state along the z direction. It is well known that when the guided cold molecules move near the point of zero electric field, they may be lost by Majorana transitions. So, to remove this molecular loss, we can add a small homogeneous bias field $\mathbf{E}_0$ along the guiding axis (i.e. the z direction) to provide a quantized axis for the guided molecules, and this bias field $\mathbf{E}_0$ along the z direction is generated by the plate capacitor with a low voltage U'.

When teflon is used as an insulating dielectric substrate, the relative dielectric constant ε_{r} and the dielectric strength of the insulating material are 2.1 and 60 kV/mm [38], respectively. The relationships between the distribution of the electric field ($E(x)|_{y=y_0}$ or $E(y)|_{x=0}$) in free space and the geometric parameters (a, b and r_0) of the charged-wire layout are studied, and the relationships between the corresponding Stark potential for CO molecules ($W(x)_{\text{Stark}}|_{y=y_0}$ or $W(y)_{\text{Stark}}|_{x=0}$) and the parameters of the charged-wire system are also studied. Here, $E(x)|_{y=y_0}$ and $W(x)_{\text{Stark}}|_{y=y_0}$ are the distribution of the electric field E and its potential W_{Stark} for CO molecules in the x direction when $y = y_0$, whereas $E(y)|_{x=0}$ and $W(y)_{\text{Stark}}|_{x=0}$ are those in the y direction when $x = 0$. Next, we will present our calculated results and the corresponding theoretical analysis.

First, the relationship between the position y_0 of the guiding center (zero electric field) and the parameters (a, b and r_0) of our guiding setup can be shown as

$$y_0 = -b + \sqrt{\left(\sqrt{a^2 + r_0^2} + a\left(-1 + \frac{\sqrt{a^2 + b^2 - r_0^2}}{\sqrt{a^2 + b^2}}\right)\right)^2 + \left(\sqrt{b^2 - r_0^2} + b\left(-1 + \frac{\sqrt{a^2 + b^2 - r_0^2}}{\sqrt{a^2 + b^2}}\right)\right)^2}. \tag{9}$$

According to Eq. (9), we calculate the dependence of the guiding-center position y_0 on the geometric parameters (a, b and r_0), and the results are shown in Fig. 2. It is clear from Fig. 2a that with the increase of the half space a (that is, the half distance between the centers of the two parallel wires), the position y_0 of the guiding center will be almost linearly increased. For example, when $r_0 = 1.0$ mm, $b = 4.0$ mm and the half space a is increased from 2 mm to 6 mm, the point y_0 of zero electric field will be lifted from 0.36 mm to 3.14 mm. Figure 3b shows that with the increase of the distance b, the position y_0 of the guiding center will be reduced rapidly. When $r_0 = 1.0$ mm, $a = 3.0$ mm and the distance b is increased from 2 mm to 20 mm, the position y_0 of the guiding center will be decreased from 1.46 mm to 0.20 mm. Figure 2c presents that with the increase of the wire radius r_0, the position y_0 of the guiding center will be slowly reduced, and when $a = 3.0$ mm, $b = 4.0$ mm and the radius r_0 is increased from 0.5 mm to 2.0 mm, the position y_0 of the guiding center will be decreased from 0.97 mm to 0.59 mm.

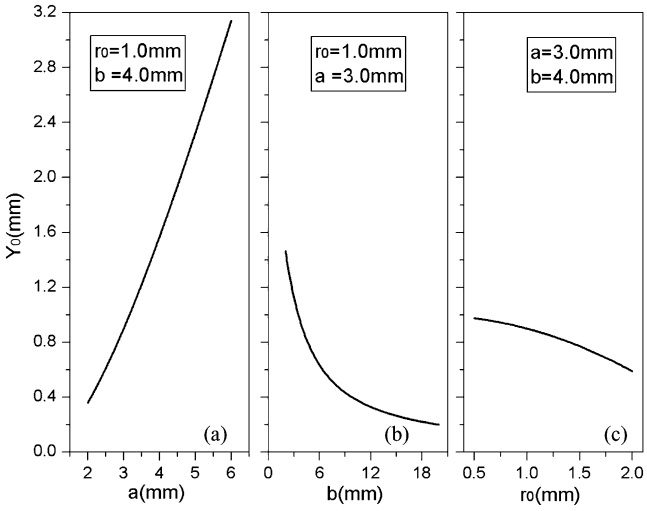

FIGURE 2 The relationships between the position y_0 of the zero electric field and **a** the half space a, **b** the distance b from the geometric center of the two wires to the metal plate, **c** the radius r_0 of the wire

Secondly, Fig. 3 shows the relationship between the electric field E and the half space a. We can see from Fig. 3a that the smaller the half space a, the larger the gradient of the electric field $E(x)$ and the larger the maximum electric field $E(x)_{\text{max}}$ (or the Stark potential $W(x)_{\text{Stark}}$) in the x direction. When $a = 3.0$ mm, $b = 3.0$ mm, $r_0 = 1.0$ mm and $U = 15$ kV, we obtain $E(x)_{\text{max}} \approx 1.6 \times 10^6$ V/m and $W(x)_{\text{Stark}} \approx 266.7$ mK. Figure 3b indicates that (1) with the reduction of the half space a, the position $(0, y_0)$ of zero electric field $E(y)$ will be lowered, but the gradient of the electric field $E(y)$ will be increased; (2) there are two maximum values in the electric field distribution $E(y)$, one is at the surface of the isolating substrate, and the other is above the zero point y_0 of the electric field. Here, the smaller one is defined as the maximum effective trapping potential ($W(y)_{\text{eff}}$) for cold molecules; (3) when $b = 3.0$ mm, $r_0 = 1.0$ mm, $U = 15$ kV and $a = 3.0$ mm, we have the maximum effective electric field $E(y)_{\text{max}} \approx 0.6 \times 10^6$ V/m and the maximum effective trapping potential $W(y)_{\text{eff}} \approx 100$ mK above $y_0 \approx 1.13$ mm, which is far higher than the transverse temperature (~ 11 mK) of cold molecules from the Stark decelerator [28]. In addition, the point y_0 of zero electric field drops from 3.64 mm to 1.13 mm with the increasing of the half space a from 3 mm to 6 mm. From the above study, we found that the electric field E and the corresponding E-field gradient scale as U/s and U/s^2, respectively, and the maximum effective trapping

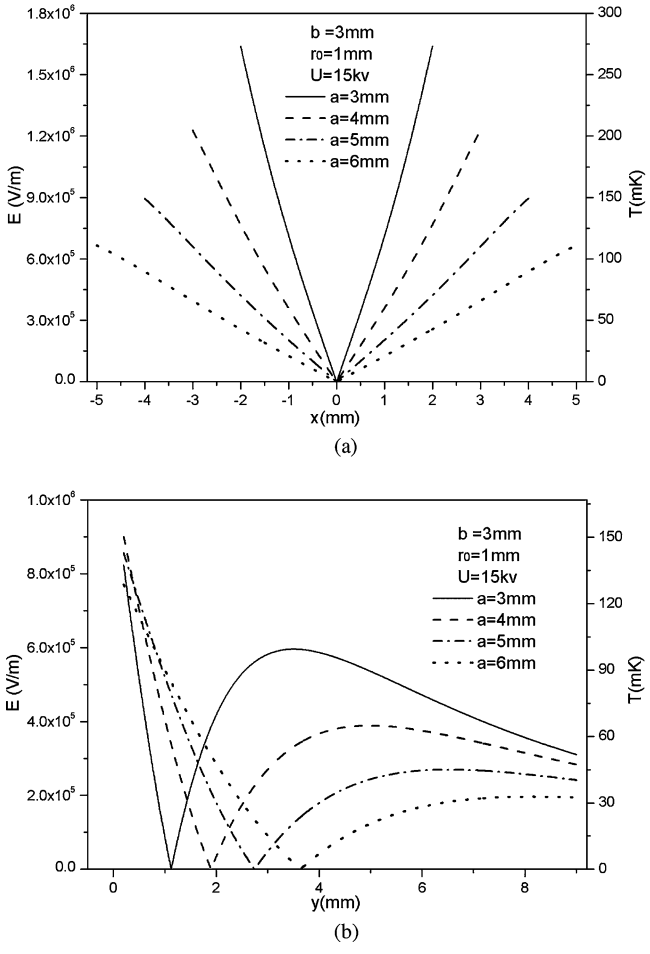

FIGURE 3 The relationships between the half space a of two wires and **a** the electric field $E(x)$ at $y = y_0$ (the corresponding trapping potential) and **b** $E(y)$ at $x = 0$ for $b = 3.0\,\text{mm}$, $r_0 = 1.0\,\text{mm}$, $U = 15\,\text{kV}$ and $a = 3.0\,\text{mm}$, 4.0 mm, 5.0 mm and 6.0 mm

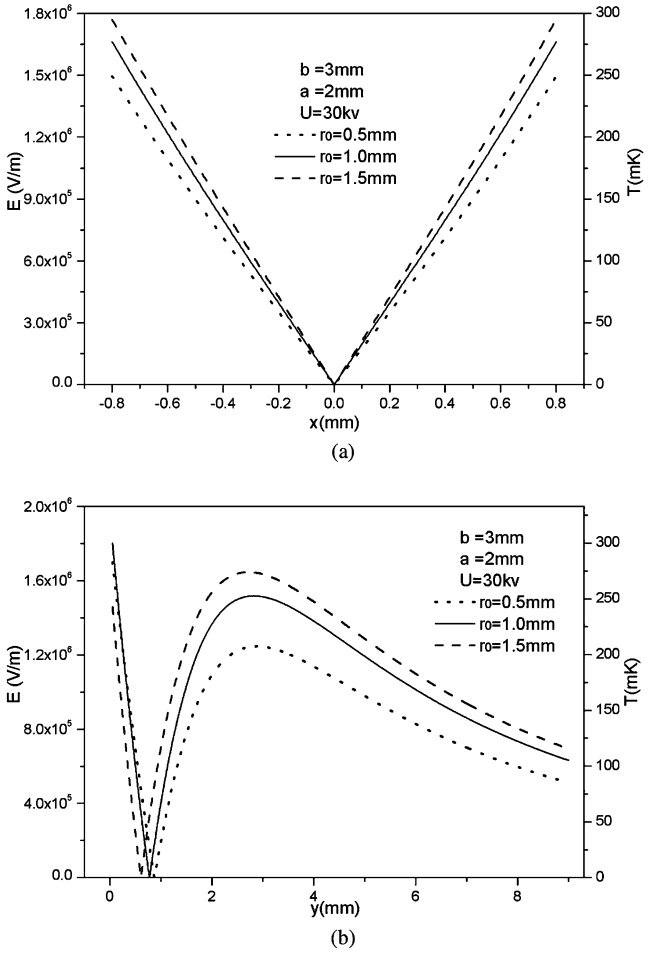

FIGURE 4 The relationships between the radius r_0 of the wire and **a** the electric field $E(x)$ at $y = y_0$ (the corresponding trapping potential) and **b** $E(y)$ at $x = 0$ for $a = 2.0\,\text{mm}$, $b = 3.0\,\text{mm}$, $U = 30\,\text{kV}$ and $r_0 = 0.5\,\text{mm}$, 1.0 mm and 1.5 mm

potential $W(y)_{\text{eff}}$ scales as U/s; here s ($s = 2a$) is the characteristic size of the guiding system.

In addition, we study the relationship between the electric field (the E-field gradient and the maximum effective trapping potential) and other parameters (b and r_0), and find that the higher the applied voltage U, and smaller the geometric parameters (a and b), and the larger the wire radius and r_0, the higher the Stark trapping potential for cold molecules. So, to obtain a higher trapping potential, we use a set of suitable parameters to calculate the distributions of the electric field and its trapping potential for cold CO molecules in the x and y directions, and the results are shown in Fig. 4. It can be seen from Fig. 4 that when $a = 2.0\,\text{mm}$, $b = 3.0\,\text{mm}$, $r_0 = 1.5\,\text{mm}$ and $U = 30\,\text{kV}$, we obtain $E(x)_{\max} \approx 1.8 \times 10^6\,\text{V/m}$ and $W(x)_{\text{Stark}} \approx 300\,\text{mK}$ at $y = y_0$, and the maximum effective electric field $E(y)_{\max} \approx 1.5 \times 10^6\,\text{V/m}$ and the maximum effective trapping potential $W(y)_{\text{eff}} \approx 250\,\text{mK}$ at $x = 0$. This shows that our two-wire system can be used to guide a Stark-decelerated, cold molecular beam with a transverse temperature of about 11 mK [28], and also can be used to guide a supersonic molecular beam with a transverse temperature of about 20 mK, which can be estimated by the divergence angle of the supersonic molecular beam.

Similarly, we also investigate the relationships between two components (F_x, F_y) of the E-field gradient force and the parameters (a, b and r_0) of the double-wire guiding system, and find that the smaller the distance b from the center of the two charged wires to the metal plate, the smaller the half space a, and the larger the radius r_0 of the wire, the greater the E-field gradient force. When $a = 2.0\,\text{mm}$, $b = 3.0\,\text{mm}$, $U = 15\,\text{kV}$ and $r_0 = 1.0\,\text{mm}$, we obtain the maximum effective trapping potential for cold molecules $W(y)_{\text{eff}} \geq 166.7\,\text{mK}$ and $F(y)_{\max} \geq 3.32 \times 10^{-22}\,\text{N}$, which is at least 728 times the gravity force exerted on CO molecules. This shows that F_y is strong enough to balance the action of the gravity force on the guided molecules.

4 Possible applications and discussion

4.1 *Some potential applications and loading of guided cold molecules*

Since our two charged wires can be fabricated on the surface of the substrate, our two-wire surface guiding scheme can be used to construct various molecular optical elements, such as a molecular funnel, a molecular beam

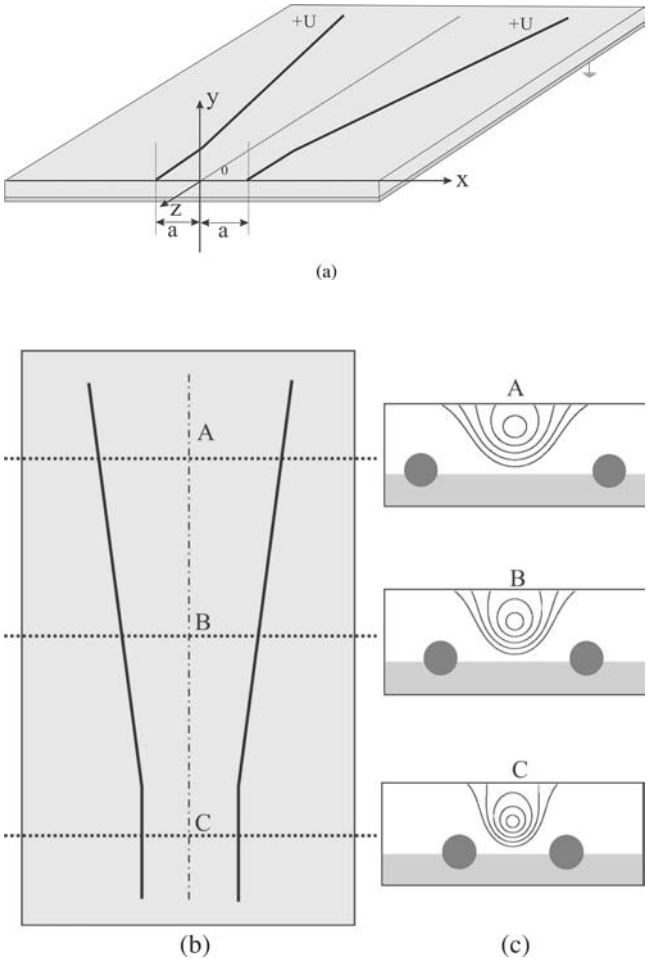

FIGURE 5 **a** 3D view of the molecular funnel scheme, **b** 2D vertical view of the molecular funnel and **c** the contours of the electric field or potential in the x–y plane (sketch map). Contours are drawn at an interval of 0.5 kV/cm and the first contour shows 0.5 kV/cm

splitter and a molecular interferometer and so on, and even to form some integrated molecular chips. For example, if the two charged wires have a fixed angle θ, and the half space a is linearly increased along the z direction, a molecular funnel using the two charged wires (see Fig. 5) can be formed. Figure 5a and b show the three-dimensional (3D) view and the 2D vertical view of the molecular funnel, respectively, and Fig. 5c shows the corresponding electric field contours or molecular funnel potentials. We can see from Fig. 5c that when the half space a between the two charged wires is linearly decreased, the radius of the electric field contour with an identical E-field value will also be reduced. This shows that the two-wire guiding system as shown in Fig. 5, as a molecular funnel, can be used to efficiently load cold molecules from an incident cold molecular beam into our two-wire guiding system or into other molecular optical elements. In addition, if an S-shaped two-wire guiding layout (as a low-pass energy filter) is used, and an effusive molecular beam is loaded into our bent two-wire guiding system by using a suitable molecular funnel, a CW colder molecular beam will be generated by the evaporative cooling of the guided molecular beam, which is similar to the experiment of Rempe's group [34, 36].

4.2 *Characteristics of our two-wire guiding scheme*

In comparison to the four-wire guiding scheme used in Refs. [34, 36], our two-wire guiding scheme has some characteristics or advantages as follows: (1) the position of the guiding center in our electrostatic tube is determined by only three geometric parameters (a, b and r_0), so it can be used to flexibly manipulate and control the guided cold molecules; (2) usually, to obtain a 2D trapping potential as high as possible, the distance $2a$ between the two wires should be as small as possible. In this case, we do not need to worry about the discharge effect between two charged wires because the electric potentials of the two charged wires are identical; (3) our two wires can be fabricated on the surface of an insulating substrate, so our scheme can be used to realize the surface guiding of cold polar molecules, and to form various surface molecular optical elements and even to develop some novel molecular chips. However, the four-wire guiding scheme [34, 36] has a higher trapping potential for cold molecules under the same geometric parameters (a and r_0) and applied high voltage, but the size of $2(a - r_0)$ in the four-wire scheme cannot be too small because it will result in a serious discharge effect between two adjacent charged wires.

5 Conclusions

In this paper, we have proposed a novel electrostatic surface guiding scheme based on the interaction between the electric dipole moment of cold polar molecules and the electrostatic field, which is generated by the combination of two parallel charged wires on the surface of the insulating substrate and the grounded metal plate, calculated the corresponding electric field distribution and analyzed the relationship between the electric field (including the trapping potential and the gradient force) and the geometric parameters of the two-wire guiding system. Our study shows that there is a point of zero electric field at the position $(0, y_0)$, and the resulting electric field distribution looks like a hollow electrostatic tube with a zero central electric field, which can be used to guide cold polar molecules in the weak-field-seeking state along the z direction, and to obtain a higher guiding efficiency.

Our electrostatic two-wire guide for cold polar molecules is different from the Keppler guide [33] and also different from the central guide with four charged wires [34–36]; it has some interesting characteristics, such as the position of the zero electric field in the electrostatic tube relying on only three parameters: the space $2a$ between the centers of the two wires, the distance b from the geometric center of the two parallel wires to the metal plate and the wire radius r_0. So, our two-wire guiding scheme cannot only be used to realize the surface guiding of cold polar molecules on the substrate, but also can be conveniently used to manipulate and control cold molecules by the above three parameters, and even to generate a continuous, cold polar molecular beam by using a bent electrostatic guide [34, 36]. Moreover, our surface guiding scheme can also be used to form various molecular optical elements, such as a molecular funnel, a molecular beam splitter and a molecular interferometer, and even to develop some integrated molecular chips.

ACKNOWLEDGEMENTS This work was supported by the National Natural Science Foundation of China (Grant Nos. 10174050, 10374029 and 10434060), the Science and Technology Commission of Shanghai Municipality (Grant No. 04DZ14009), Shanghai Priority Academic Discipline and the 211 Foundation of the Educational Ministry of China.

REFERENCES

1 J.J. Hudson, B.E. Sauer, M.R. Tarbutt, E.A. Hinds, Phys. Rev. Lett. **89**, 023003 (2002)
2 D. DeMille, F. Bay, S. Bickman, D. Kawall, D. Krause, S.E. Maxwell, L.R. Hunter, Phys. Rev. A **61**, 52 507 (2000)
3 N. Balakrishnan, A. Dalgarno, Chem. Phys. Lett. **341**, 652 (2001)
4 A.V. Avdeenkov, J.L. Bohn, Phys. Rev. A **66**, 52 718 (2002)
5 N. Balakrishnan, R.C. Forrey, A. Dalgarno, Phys. Rev. Lett. **80**, 3224 (1998)
6 J.L. Bohn, Phys. Rev. A **63**, 52 714 (2001)
7 A.V. Avdeenkov, J.L. Bohn, Phys. Rev. A **64**, 52 703 (2001)
8 P. Soldán, M.T. Cvita, J.M. Hutson, P. Honvault, J.-M. Launay, Phys. Rev. Lett. **89**, 153 201 (2002)
9 D. DeMille, Phys. Rev. Lett. **88**, 067901 (2002)
10 J.D. Weinstein, R. deCarvalho, T. Guillet, B. Friedrich, J.M. Doyle, Nature **395**, 148 (1998)
11 R. deCarvalho, J.M. Doyle, B. Friedrich, T. Guillet, J. Kim, D. Patterson, J.D. Weinstein, Eur. Phys. J. D **7**, 289 (1999)
12 A.P. Mosk, M.W. Reynolds, T.W. Hijmans, J.T.M. Walraven, Phys. Rev. Lett. **82**, 307 (1999)
13 N. Herschbach, P.J.J. Tol, W. Vassen, W. Hogervorst, G. Woestenenk, J.W. Thomsen, P. van der Straten, A. Niehaus, Phys. Rev. Lett. **84**, 1874 (2000)
14 W.I. McAlexander, E.R.I. Abraham, N.W.M. Ritchie, C.J. Williams, H.T.C. Stoof, R.G. Hulet, Phys. Rev. A **51**, R871 (1995)
15 P.D. Lett, K. Helmerson, W.D. Phillips, L.P. Ratliff, S.L. Rolston, M.E. Wagshul, Phys. Rev. Lett. **71**, 2200 (1993)
16 A.N. Nikolov, J.R. Ensher, E.E. Eyler, H. Wang, W.C. Stwalley, P.L. Gould, Phys. Rev. Lett. **84**, 246 (2000)
17 G. Zinner, T. Binnewies, F. Riehle, E. Tiemann, Phys. Rev. Lett. **85**, 2292 (2000)
18 C. Gabbanini, A. Fioretti, A. Lucchesini, S. Gozzini, M. Mazzoni, Phys. Rev. Lett. **84**, 2814 (2000)
19 A. Fioretti, D. Comparat, A. Crubellier, O. Dulieu, F. Masnou- Seeuws, P. Pillet, Phys. Rev. Lett. **80**, 4402 (1998)
20 Y. Takasu, K. Komori, K. Honda, M. Kumakura, T. Yabuzaki, Y. Takahashi, Phys. Rev. Lett. **93**, 123 202 (2004)
21 A.J. Kerman, J.M. Sage, S. Sainis, T. Bergeman, D. DeMille, Phys. Rev. Lett. **92**, 033004 (2004)
22 D. Wang, J. Qi, M.F. Stone, O. Nikolayeva, H. Wang, B. Hattaway, S.D. Gensemer, P.L. Gould, E.E. Eyler, W.C. Stwalley, Phys. Rev. Lett. **93**, 243 005 (2004)
23 S. Jochim, M. Bartenstein, A. Altmeyer, G. Hendl, S. Riedl, C. Chin, J.H. Denschlag, R. Grimm, Science **302**, 2101 (2003)
24 M. Greiner, C.A. Regal, D.S. Jin, Nature **426**, 537 (2003)
25 M.W. Zwierlein, C.A. Stan, C.H. Schunck, S.M.F. Raupach, S. Gupta, Z. Hadzibabic, W. Ketterle, Phys. Rev. Lett. **91**, 250 401 (2003)
26 H.L. Bethlem, G. Berden, G. Meijie, Phys. Rev. Lett. **83**, 1558 (1999)
27 H.L. Bethlem, A.J.A. van Roij, R.T. Jongma, G. Meijie, Phys. Rev. Lett. **88**, 13 003 (2002)
28 H.L. Bethlem, F.M.H. Crompvoets, R.T. Jongma, S.Y.T. van de Meerakker, G. Meijie, Phys. Rev. A **65**, 053416 (2002)
29 J.R. Bochinski, E.R. Hudson, H.J. Lewandowski, G. Meijer, J. Ye, Phys. Rev. Lett **91**, 243 001 (2003)
30 S.Y.T. van de Meerakker, P.H.M. Smeets, N. Vanhaecke, R.T. Jongma, G. Meijer, Phys. Rev. Lett. **94**, 023004 (2005)
31 M.R. Tarbutt, H.L. Bethlem, J.J. Hudson, V.L. Ryabov, V.A. Ryzhov, B.E. Sauer, G. Meijer, E.A. Hinds, Phys. Rev. Lett. **92**, 173 002 (2004)
32 R. Fulton, A.I. Bishop, P.F. Barker, Phys. Rev. Lett. **93**, 243 004 (2004)
33 H.J. Loesch, B. Scheel, Phys. Rev. Lett. **85**, 2709 (2000)
34 S.A. Rangwala, T. Junglen, T. Rieger, P.W.H. Pinkse, G. Rempe, Phys. Rev. A **67**, 043406 (2003)
35 T. Junglen, T. Rieger, S.A. Rangwala, P.W.H. Pinkse, G. Rempe, Phys. Rev. Lett. **92**, 223 001 (2004)
36 T. Junglen, T. Rieger, S.A. Rangwala, P.W.H. Pinkse, G. Rempe, Eur. Phys. J. D **31**(2), 1 (2004)
37 W.H. Hayt, Jr., J.A. Buck, *Engineering Electromagnetics*, 6th edn. (McGraw-Hill, New York, 2001), Chap. 5.5, p. 134
38 J.D. Kraus, D.A. Fleisch, *Electromagnetics with Applications*, 5th edn. (McGraw-Hill, New York, 1999), Chap. 7.3, p. 380